Audio Engineering Society

Convention Paper

Presented at the 142nd Convention
2017 May 20–23, Berlin, Germany

Wave Field Synthesis Driving Functions for Large-Scale Sound Reinforcement Using Line Source Arrays

Frank Schultz[1], Gergely Firtha[2], Péter Fiala[2], and Sascha Spors[3]

[1]*Audio Communication Group, TU Berlin, Germany*
[2]*Department of Networked Systems and Services, Budapest University of Technology and Economics, Hungary*
[3]*Institute of Communications Engineering, University of Rostock, Germany*

Correspondence should be addressed to Frank Schultz (frank.schultz@tu-berlin.de)

ABSTRACT

Wave field synthesis (WFS) can be used for wavefront shaping using line source arrays (LSAs) in large-scale sound reinforcement. For that the individual drivers might be electronically controlled by WFS driving functions of a virtual directional point source. From the recently introduced unified 2.5D WFS framework it is known that positions of amplitude correct synthesis (PCS) only exist along an arbitrary shaped curve—the reference curve—in front of the LSA. However, its shape can be adapted with the so called referencing function. We introduce the adaption of the referencing function along the audience line of typical concert venues for optimized wavefront shaping. This yields considerable improvements with respect to sound field's homogeneity and more convenient setups compared to previous WFS-based sound reinforcement.

1 Introduction

Wave field synthesis (WFS) using a contour of loudspeakers is a well known approach for synthesizing desired wavefronts within a target listening plane [1–3]. However, and when disregarding diffraction and spatial aliasing artifacts, amplitude correct synthesis will only be achieved along a specified reference curve within the synthesis plane [4]. Shortly after practical introduction, WFS was proposed as a large-scale sound reinforcement/public address technique [5–8].

Recently, in [9] the referencing schemes (i.e. characteristic of the referencing functions and thus resulting reference curves) of so called traditional WFS [4, 8] and revisited WFS [10, 11] were classified into a unified framework for the derivation of 2.5D WFS driving functions, i.e. the individual loudspeaker filters. For the first time the framework allows to investigate the existence and shape of reference curves—i.e. the positions of amplitude correct synthesis (PCS)—for the mentioned WFS approaches. Furthermore, with this unified framework, the derivation of arbitrary referencing functions and thus reference curves even for curved loudspeaker contours is firstly possible.

In [12] WFS was proposed as a wavefront shaping control technique using line source arrays (LSAs, [13]) for large-scale sound reinforcement. This requires spatial-aliasing free (i.e. grating lobe free) LSA radiation and individual electronic control of the LSA drivers [14]. With recent technology this can be achieved up to 10 kHz. For these LSA designs, using wavefront shaping by WFS constitutes a numerical robust and convenient forward problem solution to optimize large-scale sound reinforcement over a large audience.

In general, this requires a WFS referencing optimized for the audience locations, later referred to as the audience line due to the chosen modeling. Typically, the horizontal LSA radiation is assumed to be sufficiently homogeneous, while adapting the vertical radiation towards the audience profile of a venue. Furthermore, the WFS based sound reinforcement approach requires a wavefront shaping (originating from a virtual sound source behind the LSA) that matches the intended audience coverage w.r.t. sound pressure level (SPL). This can be realized by a virtual point source that additionally exhibits a farfield radiation pattern (FRP), here referred to as a virtual directional point source.

WFS of virtual directional sources was studied in e.g. [15–21]. In [17, 18] WFS of a virtual line piston source was discussed, whereas [21] introduced the jinc function as a virtual point source's FRP, originating from the circular piston's FRP. [19] discussed synthesis of FRPs in 2D using cylindrical harmonics, whereas [16, 20] derived FRPs of virtual sources with spherical harmonics for the 2.5D domain. [16–18, 21] used referencing w.r.t. a line parallel to the linear array, whereas [20] deployed referencing with a constant referencing function, which lead to reference curves that are dependent on the virtual source.

For the intended wavefront shaping the introduced referencing schemes and FRPs are not optimal choices. Therefore, in [12, Ch. 4] WFS of a virtual directional point source together with referencing to a specific audience position and a FRP that is adapted to the intended SPL coverage was introduced for curved and straight LSAs.

Due to the unified 2.5D WFS framework, the reference curve for a specified referencing function is known [9]. In this contribution this is utilized to improve and refine the introduced WFS based sound reinforcement of [12, Ch. 4]. We introduce so called

- *audience line adapted referencing* (applying the reference curve along the audience line) and
- *audience line adapted SPL loss* (applying a FRP of the virtual directional source to the audience line)

to even more improve the sound field's and thus sound reinforcement's quality. By claiming that, we aim at ideal allpass-like acoustic transfer functions between the LSA and all receiver points along the audience line. For the followings the assumptions are made:

- the virtual source position is far away from LSA (high frequency/farfield assumption)
- the audience positions are far away from LSA
- LSA length is much larger than the radiated wave length (in order that the LSA can be directional and the sound field prediction model is valid)
- spatial aliasing free radiation (fulfilling the spatial aliasing theorem to avoid grating lobes).

The remainder of the paper is organized as follows. Sec. 2 briefly revisits the unified 2.5D WFS approach and provides all relevant equations in general vector notation for the virtual line/point source as well as for the virtual plane wave. In Sec. 3 the virtual directional point source is introduced, whose FRP and position is to be adapted to the intended audience coverage. Sec. 4 discusses the proposed method with a practical example using numerical simulations. In Sec. 5 a brief conclusion is given.

2 Unified Framework for 2.5D WFS Driving Functions

With the speed of sound c, the temporal angular frequency ω, imaginary number j, $\mathrm{e}^{+\mathrm{j}\omega t}$ time convention applied, positional vectors in lower bold face—such as the secondary source distribution (SSD) position $\mathbf{x}_0$ (here: of the LSA drivers/sources) and the audience/listener position $\mathbf{x}$, the unit normal $\mathbf{n}(\mathbf{x}_0)$ pointing into the audience, the position $\mathbf{x}_{\mathrm{PS}}$ of the virtual point source—the 2.5D WFS driving function originating from the unified framework reads [9, (47)]

$$D(\mathbf{x}_0,\omega) = -w(\mathbf{x}_0)\sqrt{\frac{8\pi}{\mathrm{j}\frac{\omega}{c}}}\,\sqrt{d(\mathbf{x}_0)}\,\frac{\partial P(\mathbf{x},\omega)}{\partial n} \qquad (1)$$

using the referencing function $d(\mathbf{x}_0)$, which different referencing schemes can be applied for. The spatial window $w(\mathbf{x}_0)$ realizes the secondary source selection for curved SSDs [22]. The definition of the normal derivative of the sound field $P(\mathbf{x},\omega)$ is

$$\frac{\partial P(\mathbf{x},\omega)}{\partial n} = \langle \mathrm{grad}_{\mathbf{x}} P(\mathbf{x},\omega)\big|_{\mathbf{x}=\mathbf{x}_0}, \mathbf{n}(\mathbf{x}_0)\rangle \qquad (2)$$

using dot product notation $\langle\cdot,\cdot\rangle$ of vectors. The xy-plane with $x > 0$ is considered for sound reinforcement for which LSA cabinets along y-axis are deployed.

Non-focused point/line sources and plane waves that radiate towards the audience are assumed.

The unified 2.5D WFS framework introduced the concept of the local wavenumber vector for the target sound field and secondary sources. With that in [9] is stated

> "that for each receiver position $\mathbf{x}$, the synthesized sound field is mostly influenced by that SSD source $\mathbf{x}_0$, from which the emerging spherical wavefronts locally coincide with the target sound field's wavefronts, or in other words the propagation direction of a SSD element and the virtual sound field coincide. And vice versa: every point $\mathbf{x}_0$ on the SSD contributes to the total synthesized sound field mainly along a straight line, pointing from $\mathbf{x}$ towards the direction of the wave number vector $\mathbf{k}(\mathbf{x}_0)$ of the target sound field. For the case of a virtual spherical wave, this point is found in the intersection of the vector $\mathbf{x}-\mathbf{x}_{\mathrm{PS}}$ and the SSD. Although differently derived, this is a well-known result in WFS theory [4, Ch. 3]."

Furthermore, for the first time the PCS are analytical known for the virtual plane wave and line/point source and the commonly used referencing functions

- deploying (21) with a reference point $\mathbf{x}_{\mathrm{Ref}}$ [10]
- deploying $d(\mathbf{x}_0) = d_{\mathrm{Ref}} = \mathrm{const}$ [11]
- deploying $d(\mathbf{x}_0)$ such that the PCS are located at curve parallel to the SSD [2, 4, 8]

can be discussed for their resulting PCS, cf. [9] for a detailed treatment. In the following the key results of [9] that shall be worked with are presented.

2.1 Plane Wave

For the plane wave with propagating direction $\mathbf{n}_{\mathrm{PW}}$

$$P_{\mathrm{PW}}(\mathbf{x},\omega) = \mathrm{e}^{-\mathrm{j}\frac{\omega}{c}\langle \mathbf{n}_{\mathrm{PW}},\mathbf{x}\rangle} \tag{3}$$

the normal derivative (2) is given as

$$\frac{\partial P_{\mathrm{PW}}(\mathbf{x}_0,\omega)}{\partial n} = -\mathrm{j}\frac{\omega}{c}\langle \mathbf{n}_{\mathrm{PW}},\mathbf{n}(\mathbf{x}_0)\rangle P_{\mathrm{PW}}(\mathbf{x}_0,\omega). \tag{4}$$

Inserting (4) into (1) yields the driving function of the unified 2.5D WFS framework

$$D_{\mathrm{PW}}(\mathbf{x}_0,\omega) = w(\mathbf{x}_0)\sqrt{8\,\pi}\sqrt{\mathrm{j}\frac{\omega}{c}}\sqrt{d(\mathbf{x}_0)}\cdot \langle \mathbf{n}_{\mathrm{PW}},\mathbf{n}(\mathbf{x}_0)\rangle\,\mathrm{e}^{-\mathrm{j}\frac{\omega}{c}\langle \mathbf{n}_{\mathrm{PW}},\mathbf{x}_0\rangle} \tag{5}$$

with

$$w(\mathbf{x}_0) = \begin{cases} 1 & \text{if } \langle \mathbf{k}_{\mathrm{PW}}(\mathbf{x}_0),\mathbf{n}(\mathbf{x}_0)\rangle > 0 \\ 0 & \text{else} \end{cases} \tag{6}$$

and the local wavenumber of the plane wave

$$\mathbf{k}_{\mathrm{PW}}(\mathbf{x}_0) = \frac{\omega}{c}\mathbf{n}_{\mathrm{PW}}, \tag{7}$$

which in this special case is independent from $\mathbf{x}_0$. The PCS are given as [9, (28)]

$$\mathbf{x}_{\mathrm{PCS,PW}}(\mathbf{x}_0) = \mathbf{x}_0 + \mathbf{n}_{\mathrm{PW}}\cdot d(\mathbf{x}_0). \tag{8}$$

2.2 Line Source

For the line source (2D freefield Green's function) at position $\mathbf{x}_{\mathrm{LS}}$

$$P_{\mathrm{LS}}(\mathbf{x},\omega) = -\frac{\mathrm{j}}{4}H_0^{(2)}\left(\frac{\omega}{c}|\mathbf{x}-\mathbf{x}_{\mathrm{LS}}|\right), \tag{9}$$

with $H_\nu^{(2)}(\cdot)$ denoting the Hankel function of the second kind and ν-th order [23, Ch. 10], the normal derivative

$$\frac{\partial P_{\mathrm{LS}}(\mathbf{x},\omega)}{\partial n} = \frac{\langle \mathbf{x}_0-\mathbf{x}_{\mathrm{LS}},\mathbf{n}(\mathbf{x}_0)\rangle}{|\mathbf{x}_0-\mathbf{x}_{\mathrm{LS}}|}\frac{\mathrm{j}\frac{\omega}{c}H_1^{(2)}\left(\frac{\omega}{c}|\mathbf{x}_0-\mathbf{x}_{\mathrm{LS}}|\right)}{4} \tag{10}$$

is inserted into (1) yielding the driving function of the unified 2.5D WFS framework

$$D_{\mathrm{LS}}(\mathbf{x}_0,\omega) = -w(\mathbf{x}_0)\sqrt{\frac{\pi}{2}}\sqrt{\mathrm{j}\frac{\omega}{c}}\sqrt{d(\mathbf{x}_0)}\cdot \frac{\langle \mathbf{x}_0-\mathbf{x}_{\mathrm{LS}},\mathbf{n}(\mathbf{x}_0)\rangle}{|\mathbf{x}_0-\mathbf{x}_{\mathrm{LS}}|}H_1^{(2)}\left(\frac{\omega}{c}|\mathbf{x}_0-\mathbf{x}_{\mathrm{LS}}|\right) \tag{11}$$

with

$$w(\mathbf{x}_0) = \begin{cases} 1 & \text{if } \langle \mathbf{k}_{\mathrm{LS}}(\mathbf{x}_0),\mathbf{n}(\mathbf{x}_0)\rangle > 0 \\ 0 & \text{else} \end{cases} \tag{12}$$

and the local wavenumber of the line source along the SSD [9, (29)]

$$\mathbf{k}_{\mathrm{LS}}(\mathbf{x}_0) = \frac{\omega}{c}\frac{\mathbf{x}_0-\mathbf{x}_{\mathrm{LS}}}{|\mathbf{x}_0-\mathbf{x}_{\mathrm{LS}}|} \tag{13}$$

under the assumption $\frac{\omega}{c}|\mathbf{x}_0-\mathbf{x}_{\mathrm{LS}}| \gg 1$. From that the PCS

$$\mathbf{x}_{\mathrm{PCS,LS}}(\mathbf{x}_0) = \mathbf{x}_0 + \frac{\mathbf{x}_0-\mathbf{x}_{\mathrm{LS}}}{|\mathbf{x}_0-\mathbf{x}_{\mathrm{LS}}|}\cdot d(\mathbf{x}_0) \tag{14}$$

are derived [9, (30)].

The 3 dB/octave temporal lowpass characteristic of the ideal line source in the farfield can be compensated in the driving function (11) with the additional filter $H_{\mathrm{3dBHP}} = \sqrt{\mathrm{j}\,\omega}$ to obtain a flat temporal spectrum.

2.3 Point Source

For the point source (3D freefield Green's function) at position $\mathbf{x}_{\mathrm{PS}}$

$$P_{\mathrm{PS}}(\mathbf{x},\omega) = \frac{\mathrm{e}^{-\mathrm{j}\frac{\omega}{c}|\mathbf{x}-\mathbf{x}_{\mathrm{PS}}|}}{4\pi|\mathbf{x}-\mathbf{x}_{\mathrm{PS}}|} \tag{15}$$

the normal derivative if $\frac{\omega}{c}|\mathbf{x}_0-\mathbf{x}_{\mathrm{PS}}| \gg 1$ (i.e. the high frequency/far field gradient approximation) is given as

$$\frac{\partial P_{\mathrm{PS}}(\mathbf{x},\omega)}{\partial n} = -\mathrm{j}\frac{\omega}{c}\frac{\langle \mathbf{x}_0-\mathbf{x}_{\mathrm{PS}}, \mathbf{n}(\mathbf{x}_0)\rangle}{|\mathbf{x}_0-\mathbf{x}_{\mathrm{PS}}|} P_{\mathrm{PS}}(\mathbf{x}_0,\omega). \tag{16}$$

Inserting (16) into (1) yields the driving function of the unified 2.5D WFS framework

$$D_{\mathrm{PS}}(\mathbf{x}_0,\omega) = w(\mathbf{x}_0)\sqrt{\frac{1}{2\pi}}\sqrt{\mathrm{j}\frac{\omega}{c}}\sqrt{d(\mathbf{x}_0)}\cdot \frac{\langle \mathbf{x}_0-\mathbf{x}_{\mathrm{PS}}, \mathbf{n}(\mathbf{x}_0)\rangle}{|\mathbf{x}_0-\mathbf{x}_{\mathrm{PS}}|}\frac{\mathrm{e}^{-\mathrm{j}\frac{\omega}{c}|\mathbf{x}_0-\mathbf{x}_{\mathrm{PS}}|}}{|\mathbf{x}_0-\mathbf{x}_{\mathrm{PS}}|} \tag{17}$$

with

$$w(\mathbf{x}_0) = \begin{cases} 1 & \text{if } \langle \mathbf{k}_{\mathrm{PS}}(\mathbf{x}_0), \mathbf{n}(\mathbf{x}_0)\rangle > 0 \\ 0 & \text{else} \end{cases} \tag{18}$$

and the local wavenumber of the point source along the SSD

$$\mathbf{k}_{\mathrm{PS}}(\mathbf{x}_0) = \frac{\omega}{c}\frac{\mathbf{x}_0-\mathbf{x}_{\mathrm{PS}}}{|\mathbf{x}_0-\mathbf{x}_{\mathrm{PS}}|}. \tag{19}$$

From that the PCS are given as [9, (34)]

$$\mathbf{x}_{\mathrm{PCS,PS}}(\mathbf{x}_0) = \mathbf{x}_0 + (\mathbf{x}_0-\mathbf{x}_{\mathrm{PS}})\cdot\frac{d(\mathbf{x}_0)}{|\mathbf{x}_0-\mathbf{x}_{\mathrm{PS}}|-d(\mathbf{x}_0)}. \tag{20}$$

When comparing (17) with the driving function [12, (2.137)]—which originates from the first stationary phase approximation, cf. [4, (3.9-3.11)]—we can identify the referencing function (cf. [9, (31)])

$$d(\mathbf{x}_0) = \frac{|\mathbf{x}_0-\mathbf{x}_{\mathrm{PS}}|\cdot|\mathbf{x}_{\mathrm{Ref}}-\mathbf{x}_0|}{|\mathbf{x}_0-\mathbf{x}_{\mathrm{PS}}|+|\mathbf{x}_{\mathrm{Ref}}-\mathbf{x}_0|} \tag{21}$$

using a fixed reference point $\mathbf{x}_{\mathrm{Ref}}$. The PCS are then given as

$$\mathbf{x}_{\mathrm{PCS,PS,SPA1}}(\mathbf{x}_0) = \mathbf{x}_0 + \frac{\mathbf{k}_{\mathrm{PS}}(\mathbf{x}_0)}{\frac{\omega}{c}}|\mathbf{x}_{\mathrm{Ref}}-\mathbf{x}_0|. \tag{22}$$

In [12, Ch. 4] this referencing scheme was used for WFS of a virtual directional point source as a sound reinforcement application for large venues, exemplarily setting the reference point $\mathbf{x}_{\mathrm{Ref}}$ approximately in the middle of the audience line. From (22) it is obvious that this referencing scheme is not the optimal choice when PCS along the audience line are intended, cf. the PCS as red curve in Fig. 2b.

Therefore, we propose to adapt the referencing function $d(\mathbf{x}_0)$ such that $\mathbf{x}_{\mathrm{PCS,PS}}(\mathbf{x}_0)$ (20) are located along the audience line to ensure amplitude correct synthesis exactly there, cf. Fig. 2c. In fact, having knowledge of (20) and adjusting $d(\mathbf{x}_0)$—as one main result of [9]—for the first time allows to improve the proposed approach in [12, Ch. 4]. Furthermore, to control the SPL loss over the audience line, the usage of a virtual directional point source was proposed in [12], which is refined in the next section.

3 Virtual Directional Point Source

The 2.5D WFS unified framework driving function of a virtual directional point source is derived from (17) by adding an LSA source dependent gain factor $g_{\mathrm{PS,FRP}}(\mathbf{x}_{0,i})$ (cf. [16, (10)], [21, (4)], [12, (4.33)]) and is thus generally given as

$$D_{\mathrm{PS,FRP}}(\mathbf{x}_{0,i},\omega) = w(\mathbf{x}_{0,i})\sqrt{\frac{1}{2\pi}}\sqrt{\mathrm{j}\frac{\omega}{c}}\sqrt{d(\mathbf{x}_{0,i})}\cdot g_{\mathrm{PS,FRP}}(\mathbf{x}_{0,i})\cdot\frac{\langle \mathbf{x}_{0,i}-\mathbf{x}_{\mathrm{PS}}, \mathbf{n}(\mathbf{x}_{0,i})\rangle}{|\mathbf{x}_{0,i}-\mathbf{x}_{\mathrm{PS}}|}\frac{\mathrm{e}^{-\mathrm{j}\frac{\omega}{c}|\mathbf{x}_{0,i}-\mathbf{x}_{\mathrm{PS}}|}}{|\mathbf{x}_{0,i}-\mathbf{x}_{\mathrm{PS}}|}. \tag{23}$$

For the discretized, finite-length LSA the index i for the i-th LSA source is introduced here.

In [12, Ch. 4] it was proposed to calculate a reference farfield radiation pattern (FRP) of the virtual directional point source w.r.t. a chosen reference point $\mathbf{x}_{\mathrm{Ref}}$. The distance ratio between $|\mathbf{x}_{\mathrm{Ref}}-\mathbf{x}_{\mathrm{PS}}|$ and $|\mathbf{x}-\mathbf{x}_{\mathrm{PS}}|$ can be expressed in terms of the level [12, (4.34)]

$$H_{\mathrm{PS,FRP}}(\varphi_{\mathbf{x}}) = DD_{\mathrm{dB}}\cdot\log_{10}\left(\frac{|\mathbf{x}_{\mathrm{Ref}}-\mathbf{x}_{\mathrm{PS}}|}{|\mathbf{x}-\mathbf{x}_{\mathrm{PS}}|}\right), \tag{24}$$

where the factor DD_{dB} controls the effective SPL loss over the audience if $\mathbf{x}_{\mathrm{Ref}}$ and $\mathbf{x}$ are audience positions. For $DD_{\mathrm{dB}} = -20$ dB no SPL loss over the whole audience is obtained (cf. Fig. 6), $DD_{\mathrm{dB}} = -10$ dB realizes a 3 dB SPL loss w.r.t. the considered distance ratio (cf. Fig. 5), whereas $DD_{\mathrm{dB}} = 0$ dB defines an

omni-directional FRP within the resulting spatial region (cf. Fig. 3). Any other suitable 'distance ratio to dB mapping' can be easily adapted (cf. e.g. the array processing approach of *d&b audiotechnik ArrayCalc*[1]). However, all choices yield FRPs for an audience line adapted SPL loss, which is of most practical importance for LSA based sound reinforcement.

For the chosen geometry and setup, the corresponding radiation angle $\varphi_{\mathbf{x}}$ is given as [12, (4.35)]

$$\varphi_{\mathbf{x}} = \operatorname{acos}\left(\langle \frac{\mathbf{x}-\mathbf{x}_{\mathrm{PS}}}{|\mathbf{x}-\mathbf{x}_{\mathrm{PS}}|}, (1,0,0)^{\mathrm{T}}\rangle\right) \cdot \begin{cases} (-1) & \text{if } \langle (0,0,1)^{\mathrm{T}}, \frac{\mathbf{x}-\mathbf{x}_{\mathrm{PS}}}{|\mathbf{x}-\mathbf{x}_{\mathrm{PS}}|} \times (1,0,0)^{\mathrm{T}}\rangle > 0 \\ (+1) & \text{else} \end{cases}, \tag{25}$$

w.r.t. the reference direction into x-axis, cf. Fig. 1.

The gain factor $g(\mathbf{x}_{0,i})$ of the WFS driving function requires the FRP's gain w.r.t. the secondary source position's angle [12, (4.36)]

$$\varphi_{\mathbf{x}_{0,i}} = \operatorname{acos}\left(\langle \frac{\mathbf{x}_{0,i}-\mathbf{x}_{\mathrm{PS}}}{|\mathbf{x}_{0,i}-\mathbf{x}_{\mathrm{PS}}|}, (1,0,0)^{\mathrm{T}}\rangle\right) \cdot \begin{cases} (-1) & \text{if } \langle (0,0,1)^{\mathrm{T}}, \frac{\mathbf{x}_{0,i}-\mathbf{x}_{\mathrm{PS}}}{|\mathbf{x}_{0,i}-\mathbf{x}_{\mathrm{PS}}|} \times (1,0,0)^{\mathrm{T}}\rangle > 0 \\ (+1) & \text{else} \end{cases}. \tag{26}$$

Since, the estimated $\varphi_{\mathbf{x}}$ and the required $\varphi_{\mathbf{x}_{0,i}}$ typically not coincide, an interpolation is performed. Using the FRP $H_{\mathrm{PS,FRP}}(\varphi_{\mathbf{x}})$ in dB and $\varphi_{\mathbf{x}}/\varphi_{\mathbf{x}_{0,i}}$ in degree a cubic spline interpolation yields $H_{\mathrm{PS,FRP}}(\varphi_{\mathbf{x}_{0,i}})$. The corresponding linear gain factor [12, (4.37)]

$$g_{\mathrm{PS,FRP}}(\mathbf{x}_{0,i}) = 10^{\frac{H_{\mathrm{PS,FRP}}(\varphi_{\mathbf{x}_{0,i}})}{20}} \tag{27}$$

is then applied in (23).

The position $\mathbf{x}_{\mathrm{PS}}$ of the virtual point source should be set into the intersection of the two lines [12, (4.38)]

$$\mathbf{x}_{\mathrm{Aud},m=1} - \mathbf{x}_{0,i=LN} \qquad \mathbf{x}_{\mathrm{Aud},m=M} - \mathbf{x}_{0,i=1}, \tag{28}$$

i.e. from a vector that starts from the nearest audience point $m = 1$ to the lowest LSA source $i = LN$ and from a vector that starts from the farthest audience point $m = M$ to the top LSA source $i = 1$, cf. Fig. 1. This requires careful curving of the LSA such that the LSA cabinets cover the intended audience. A progressively curved scheme [24, 25] is adequate for the given example, for which an appropriate tilt angle and spiral opening angle ensures sufficient mechanical coverage. The angles and the rigging height could be conveniently chosen such that the unit normals of the LSA sources and the normal vectors of (28) ideally coincide, i.e. (cf. Fig. 1)

$$\begin{aligned} \mathbf{n}(\mathbf{x}_{0,i=LN}) &= \frac{\mathbf{x}_{\mathrm{Aud},m=1} - \mathbf{x}_{0,i=LN}}{|\mathbf{x}_{\mathrm{Aud},m=1} - \mathbf{x}_{0,i=LN}|} \\ \mathbf{n}(\mathbf{x}_{0,i=1}) &= \frac{\mathbf{x}_{\mathrm{Aud},m=M} - \mathbf{x}_{0,i=1}}{|\mathbf{x}_{\mathrm{Aud},m=M} - \mathbf{x}_{0,i=1}|}, \end{aligned} \tag{29}$$

with ideally equidistant spatial sampling of the LSA source's impact points along the audience line, cf. [26]. The latter can hardly be realized in practice due to rigging constraints. With appropriate LSA curving and using the intersection of the vectors in (28) for $\mathbf{x}_{\mathrm{PS}}$ ideally the local wavenumber vector

$$\frac{\mathbf{k}_{\mathrm{PS}}(\mathbf{x}_{0,i=LN})}{\frac{\omega}{c}} = \mathbf{n}(\mathbf{x}_{0,i=LN}) \quad \frac{\mathbf{k}_{\mathrm{PS}}(\mathbf{x}_{0,i=1})}{\frac{\omega}{c}} = \mathbf{n}(\mathbf{x}_{0,i=1}) \tag{30}$$

coincides with the specified LSA source's normal vectors. This in turn yields PCS only on the audience line, when adapting the referencing function towards the audience. By doing so, large contributions of sources whose PCS are not part of the audience line is avoided, consequently avoiding high SPL in non-coverage zones. Note that from (30) the property $\frac{\mathbf{k}_{\mathrm{PS}}(\mathbf{x}_{0,i})}{\frac{\omega}{c}} = \mathbf{n}(\mathbf{x}_{0,i})$ holds for an arc curved LSA.

4 Application Example: WFS with LSA

This section shall demonstrate the proposed approach of (i) choosing a WFS referencing scheme combined with (ii) choosing a virtual point source's FRP for audience adapted SPL coverage by means of numerical simulations. For (i) referencing w.r.t. a single reference point $\mathbf{x}_{\mathrm{Ref}}$ is compared against the audience line adapted referencing. For (ii) the introduced factor DD_{dB} (24) is varied, yielding different audience line adapted SPL losses.

4.1 Setup

For the simulations a typical open-air amphitheater situation is considered (resembling the Waldbühne in Berlin[2]). It exhibits 4 audience zones, i.e. the floor and three stands, that may be simplified by the profile within the xy-plane $\mathbf{x}_{\mathrm{Aud}}/\mathrm{m} = (10,0,0)^{\mathrm{T}} \overset{\mathrm{Floor}}{\rightarrow}$

[1] http://www.dbaudio.com/en/systems/details/arraycalc.html

[2] http://www.waldbuehne-berlin.de/

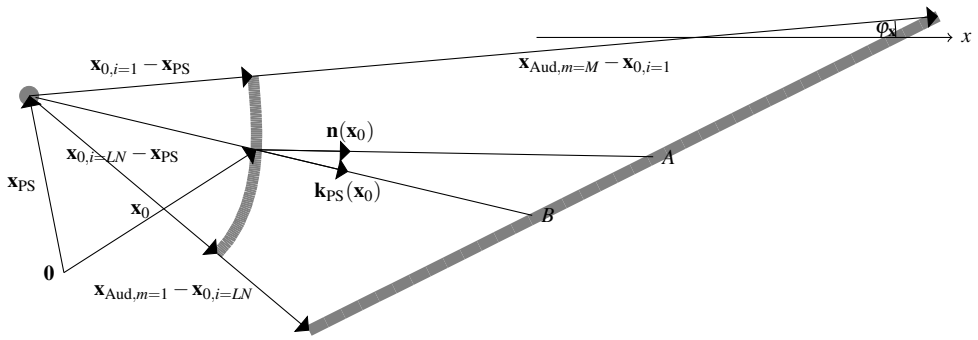

Fig. 1: Geometry for a virtual (directional) point source, a curved line source array (LSA) and an audience line within a plane (in gray, not to scale). For the here shown setup the local wavenumber vectors $\mathbf{k}_{\mathrm{PS}}(\mathbf{x}_{0,i=1})/\frac{\omega}{c} = \mathbf{n}(\mathbf{x}_{0,i=1})$ and $\mathbf{k}_{\mathrm{PS}}(\mathbf{x}_{0,i=LN})/\frac{\omega}{c} = \mathbf{n}(\mathbf{x}_{0,i=LN})$ correspond with the normals of the uppermost and lowermost LSA source, respectively. On the other hand, the vectors $\mathbf{k}_{\mathrm{PS}}(\mathbf{x}_0)$ and $\mathbf{n}(\mathbf{x}_0)$ for the specified position $\mathbf{x}_0$ are not coincident. In this case the LSA source at $\mathbf{x}_0$ contributes most to the WFS sound field along line B, whereas its on-axis response contributes along line A.

$(30,1.5,0)^{\mathrm{T}} \overset{\text{1st St}}{\rightarrow} (60,10,0)^{\mathrm{T}} \overset{\text{2nd St}}{\rightarrow} (85,20,0)^{\mathrm{T}} \overset{\text{3rd St}}{\rightarrow} (110,30,0)^{\mathrm{T}}$, setting the stage edge at $x = 0$ m. Thus, $\mathbf{x}_{m=1}/\mathrm{m} = (10,0,0)^{\mathrm{T}}$ and $\mathbf{x}_{m=M}/\mathrm{m} = (110,30,0)^{\mathrm{T}}$ is defined. For this venue, sound reinforcement requires an extreme long-throw LSA application. No delay lines and no side/front fills are considered for simplicity. The reference point $\mathbf{x}_{\mathrm{Ref}}/\mathrm{m} = (60,10,0)^{\mathrm{T}}$ is used. Speed of sound $c = 343\,\mathrm{m/s}$ is chosen.

A spirally curved LSA is setup following the algorithm in [25]. The tilt angle is set to 9 deg and the spiral opening angle to 40 deg. Note that this setting does not strictly fulfill (29). The LSA consists of $N = 18$ LSA cabinets of individual height $\Delta y_{\mathrm{Cabinet}} = \frac{8}{N}$ m. Each LSA cabinet has $L = 15$ line pistons drivers [27] for the high frequencies (HF, > 1 kHz). The sampling distance between line pistons for a straight LSA is then $\Delta y_{\mathrm{Piston}} = \frac{8}{LN}$ m = 1.1665 inch. The line piston height is 1 inch, thus realizing an active radiating factor of ARF=0.85 [27]. This is in line with several modern LSAs. The paper only discusses the HF characteristics of the LSA radiation. The feasible rigging height of the LSA is set to $\mathbf{x}_{\mathrm{T}}/\mathrm{m} = (0,13.5,0)^{\mathrm{T}}$.

For the chosen venue and LSA curving, the position of the virtual directional point source in the intersection of (28) is estimated to $\mathbf{x}_{\mathrm{PS}}/\mathrm{m} = (-11.8,11.7,0)^{\mathrm{T}}$. The venue profile, virtual point source position and LSA setup are depicted in Fig. 2c.

The prediction of the sound field $P_{\mathrm{WFS,LSA}}(\mathbf{x},\omega)$ happens with the high-frequency approximated boundary element method (HF-BEM) kernel [12, (4.29)]. All simulations were performed in the `aes142nd` branch of the Matlab based, open source *Line Source Array Prediction Toolbox* (LSAPT)[3], following the reproducible research paradigm.

4.2 Evaluation Strategy

The technical quality of the resulting sound field $P_{\mathrm{WFS,LSA}}(x,y,\omega)$ and thus sound reinforcement is evaluated by means of different visualizations and technical measures, cf. [28]. The widely adopted plot "SPL over the xy-plane for individual frequencies f" provides a fast and convenient overview on how the generated 'beam' (i.e. wavefront shape) covers the intended audience line, here exemplarily given for $f = 4$ kHz. The so called position index plot (PIP) provides a convenient overview for the magnitude frequency response (x-axis) over all audience positions (y-axis). Here both, the SPL and the PIP are also used to indicate deviation measures between the sound fields of the virtual point source and the one synthesized with WFS.

A further quality measure for the obtained SPL distribution per audience position m is calculated as

$$L_{p,\mathrm{Aud},m} = \underset{\omega}{\mathscr{Q}_q}\left[20\log_{10}\left(P_{\mathrm{WFS,LSA}}(\mathbf{x}_{\mathrm{Aud},m},\omega)\right)\right]. \tag{31}$$

The operator $\mathscr{Q}_q[\cdot]$ calculates the $q = \{0.05, 0.25, 0.50, 0.75, 0.95\}$ quantiles over the radial frequency ω. In

[3] `https://bitbucket.org/fs446/lsapt/branch/aes142nd`

the present simulations the range $1\,\mathrm{kHz} < f < 10\,\mathrm{kHz}$ is used. This distribution measure provides a convenient overview for the SPL loss over the audience line as well as the magnitude response variation over the audience line in terms of the considered quantiles.

All levels are normalized to the amplitude of the virtual (directional) point source at $\mathbf{x}_{\mathrm{Ref}}/\mathrm{m} = (60, 10, 0)^{\mathrm{T}}$, thus they can be regarded as relative SPLs w.r.t. an arbitrary reference SPL. Note that by doing so, no conclusions can be drawn for the required electrical power driving the LSA. Refer to [12] for a concise treatment. However, in the Fig. 4e and Fig. 4f the amplitude spectra of the WFS driving function over the LSA sources—the so called driving function index plot (DFIP)— for DD_{dB}=0 dB are depicted from which relative power requirements can be estimated for the specified case.

4.3 Results

In the following we shall discuss that the audience line adapted referencing scheme is superior to the single receiving point referencing for the intended LSA application based upon the given simulations.

4.3.1 Referencing Schemes / Audience Line Adapted Referencing

Fig. 2 shows the SPL_{xy} plot of the virtual point source and the two considered referencing schemes.

In Fig. 2b the referencing scheme (21) with $\mathbf{x}_{\mathrm{Ref}}/\mathrm{m} = (60, 10, 0)^{\mathrm{T}}$ yields the PCS (22) as red curve. For reference points far away from the LSA the PCS have a similarly curved shape as the LSA itself. For the subsequent Fig. 3, Fig. 4, Fig. 5, Fig. 6 this referencing scheme is depicted in the **left** subfigures.

On the other hand, Fig. 2c depicts the case of referencing adapted to the audience line, here the red PCS line overlays the black audience line. For that (20) must be (numerically) solved for $d(\mathbf{x}_0)$ such that $\mathbf{x}_{\mathrm{PCS,PS}}(\mathbf{x}_0)$ coincides with the audience line $\mathbf{x}_{\mathrm{Aud}}$. The estimated $d(\mathbf{x}_0)$ is then put into the unified WFS driving function (17) instead of (21). For the subsequent Fig. 3, Fig. 4, Fig. 5, Fig. 6 this novel referencing scheme is depicted in the **right** subfigures.

The case for WFS of a virtual, omni-directional point source (i.e. DD_{dB}=0 dB) with the considered LSA is depicted in Fig. 3. Due to the different referencing schemes slightly different wavefront shapes result in Fig. 3a vs. Fig. 3b, especially close to the LSA. The 6 dB isobars clearly indicate spatial truncation (diffraction) artifacts due to the finite-length LSA setup. In Fig. 3c and Fig. 3d the deviation of the synthesized sound field from the sound field of the ideal point source is given. The audience line adapted referencing shown in Fig. 3d exhibits less deviation, whereas the error in the reference point approach is comparably larger at audience positions close to the LSA. The error at top audience positions very far away from the LSA is due to the diffraction artifacts, of course occurring at both referencing schemes. The trend of the SPL along the audience line for 4 kHz is shown in Fig. 3e vs. Fig. 3f. This supports the SPLxy plots and indicates that only close positions are affected by the referencing scheme difference for the chosen parameters.

In Fig. 4 the PIP and the error PIP between the sound field of the ideal point source and the synthesized one are depicted. The PIP indicates smooth magnitude responses along the audience line together with the expected SPL loss of the virtual point source over distance $|\mathbf{x}_{\mathrm{Aud}} - \mathbf{x}_{\mathrm{PS}}|$. The frequency dependent error measures (ideal point source vs. synthesized point source) Fig. 4c vs. Fig. 4d indicate that the error is generally smaller for the audience line adapted referencing.

4.3.2 Virtual Directional Point Source / Audience Adapted SPL Loss

Fig. 3f indicates an SPL loss of about 13.5 dB from the nearest (near stage) to the farthest (last row in 4th stand) audience position when using WFS with the virtual point source to control the LSA. Based on an assumed median SPL at the front of house position this is an approx. $\pm$6 dB deviation for these extreme audience positions. In many applications this is not desired and less SPL loss and less deviation will be pursued. This can be achieved with WFS of the introduced virtual directional point source that adapts the FRP and by that the SPL loss to the audience line. Two straightforward approaches shall be discussed. Note that the LSA curving remains unaltered while changing electronic control in order to do this.

In Fig. 5 and Fig. 6 the audience adapted SPL loss for DD_{dB}=-10 dB and DD_{dB}=-20 dB, respectively is shown. The resulting dynamic range of the DFIPs (i.e. gain for lowest HF frequency in lowest LSA source vs. gain for highest HF frequency in top LSA source) are about 17 dB for Fig. 5(left), 20 dB for Fig. 5(right), 24 dB for Fig. 6(left) and 27 dB for Fig. 6(right).

Except for very far audience positions (large error

due to diffraction artifacts) the SPL loss is reduced to about 5 dB for the case DD_{dB}=-10 dB. Here the chosen DD_{dB} results in a 3 dB level loss over the distance $|\mathbf{x}_{\mathrm{Aud}} - \mathbf{x}_{\mathrm{PS}}|$. The SPL in the *xy*-plane shows the corresponding wavefront shape, very often practically approached in similar sound reinforcement situations. The PIP indicates smooth magnitude responses with the intended level loss over audience. The distribution measure confirms very flat magnitude responses and the desired level loss. With the factor DD_{dB}=-20 dB used for Fig. 6 no SPL loss over the audience line is realized (except again the far positions). Thus, the audience line, the PCS and the 0 dB SPL isobar are congruent as depicted in Fig. 6b. Together with the audience line adapted referencing this audience line adapted SPL loss can yield an extraordinary flat magnitude spectrum within ± 1 dB range, cf. Fig. 6f.

A combination of different SPL losses over the audience line—starting with no SPL loss for near positions, 3 dB for middle positions and 6 dB for farthermost positions, termed *composite SPL target*—is proposed in [29], achieved by pure mechanical control (i.e. LSA curving) and no electronic control. This can be seen as a local plane wave approximation/synthesis, where $\mathbf{n}_{\mathrm{PW}}(\mathbf{x}_{0,i}) = \mathbf{n}(\mathbf{x}_{0,i})$ is approached. With WFS of a virtual directional point source this specific SPL loss scheme can be easily realized. However, a spatial aliasing free LSA is required for doing that [14, 27].

It is worth noting that instead of the virtual directional point source, the virtual directional line source can be used as well for the indented adaptation of the SPL along the audience line. Since only the resulting level along the audience line is of interest, the level loss of the ideal line source as well as that of the synthesized one are not of importance. Thus, only the factor DD_{dB} must be differently adapted for desired SPL loss when using a virtual directional line source.

Due to the local wavenumber vector and the resulting PCS the virtual single plane wave model is not an appropriate choice for the intended application.

5 Conclusion

The audience line adapted referencing scheme together with the audience line adapted sound pressure level loss realized by controlling the farfield radiation pattern of a virtual directional (non-focused) point source was introduced for wave field synthesis with line source arrays in large-scale sound reinforcement.

For spatial aliasing free arrays this yields a forward problem solution for optimized audience coverage of large venues. The points of amplitude correct wavefront synthesis along the audience line—as an adapted referencing scheme for the intended application—are found by applying the local wavenumber concept from the recently introduced unified synthesis framework.

The results indicate an improved technical quality of the synthesized wavefronts with less degrees of freedom compared to earlier approaches. The audience line adapted referencing is superior to referencing to a specific reference point.

References

[1] Berkhout, A.J. (1988): "A holographic approach to acoustic control." In: *J. Audio Eng. Soc.*, **36**(12):977–995.

[2] Berkhout, A.J.; de Vries, D.; Vogel, P. (1993): "Acoustic control by Wave Field Synthesis." In: *J. Acoust. Soc. Am.*, **93**(5):2764–2778.

[3] de Vries, D. (2009): *Wave Field Synthesis – AES Monograph*. New York: Audio Eng. Soc.

[4] Start, E.W. (1997): *Direct Sound Enhancement by Wave Field Synthesis*. Ph.D. thesis, Delft University of Technology.

[5] Berkhout, A.J.; Vogel, P.; de Vries, D. (1992): "Use of wave field synthesis for natural reinforced sound." In: *Proc. of 92nd Audio Eng. Soc. Conv., Vienna*, #3299.

[6] de Vries, D.; Start, E.W.; Valstar, V.G. (1994): "The Wave Field Synthesis concept applied to sound reinforcement: Restrictions and solutions." In: *Proc. of 96th Audio Eng. Soc. Conv., Amsterdam*, #3812.

[7] Start, E.W. (1996): "Application of curved arrays in Wave Field Synthesis." In: *Proc. of 100th Audio Eng. Soc. Conv., Copenhagen*, #4143.

[8] de Vries, D. (1996): "Sound reinforcement by wavefield synthesis: Adaptation of the synthesis operator to the loudspeaker directivity characteristics." In: *J. Audio Eng. Soc.*, **44**(12):1120–1131.

[9] Firtha, G.; Fiala, P.; Schultz, F.; Spors, S. (2017): "Improved Referencing Schemes for 2.5D Wave Field Synthesis Driving Functions." In: *IEEE/ACM Trans. Audio, Speech, Language Process.*, **x**(accepted for publication):xxx–xxx.

[10] Spors, S.; Rabenstein, R.; Ahrens, J. (2008): "The theory of Wave Field Synthesis revisited." In: *Proc. of 124th Audio Eng. Soc. Conv., Amsterdam*, #7358.

[11] Ahrens, J. (2012): *Analytic Methods of Sound Field Synthesis*. Heidelberg: Springer.

[12] Schultz, F. (2016): *Sound Field Synthesis for Line Source Array Applications in Large-Scale Sound Reinforcement*. Ph.D. thesis, University of Rostock, urn:nbn:de:gbv:28-diss2016-0078-1.

[13] Urban, M.; Heil, C.; Baumann, P. (2003): "Wavefront Sculpture Technology." In: *J. Audio Eng. Soc.*, **51**(10):912–932.

[14] Schultz, F.; Rettberg, T.; Spors, S. (2014): "On spatial-aliasing-free sound field reproduction using finite length line source arrays." In: *Proc. of 137th Audio Eng. Soc. Conv., Los Angeles*, #9098.

[15] Jacques, R.; Albrecht, B.; Melchior, F.; de Vries, D. (2005): "An approach for multichannel recording and reproduction of sound source directivity." In: *Proc. of 119th Audio Eng. Soc. Conv., New York*, #6554.

[16] Corteel, E. (2007): "Synthesis of directional sources using Wave Field Synthesis, possibilities, and limitations." In: *EURASIP J. on Adv. in Sig. Proc.*, (90509).

[17] Romoli, L.; Peretti, P.; Palestini, L.; Cecchi, S.; Piazza, F. (2008): "A new approach to digital directivity control of loudspeakers line arrays using wave field synthesis theory." In: *Proc. of the Intl. Workshop on Acoustic Signal Enhancement (IWAENC), Seattle*, #9022.

[18] Peretti, P.; Romoli, L.; Palestini, L.; Cecchi, S.; Piazza, F. (2008): "Wave field synthesis: Practical implementation and application to sound beam digital pointing." In: *Proc. of 125th Audio Eng. Soc. Conv., San Francisco*, #7618.

[19] Franck, A.; Rath, M.; Sladeczek, C.; Brix, S. (2012): "Efficient rendering of directional sound sources in wave field synthesis." In: *Proc. of 40th Intl. Audio Eng. Soc. Conf., Helsinki*.

[20] Ahrens, J.; Spors, S. (2012): "Wave Field Synthesis of a sound field described by spherical harmonics expansion coefficients." In: *J. Acoust. Soc. Am.*, **131**(3):2190–2199.

[21] Romoli, L.; Cecchi, S.; Peretti, P.; Piazza, F. (2015): "Real-time implementation and performance evaluation of digital control for loudspeakers line arrays." In: *Applied Acoustics*, **97**:121–132.

[22] Spors, S. (2007): "Extension of an analytic secondary source selection criterion for wave field synthesis." In: *Proc. of the 123rd Audio Eng. Soc. Conv., New York*.

[23] Olver, F.W.J.; Lozier, D.W.; Boisvert, R.F.; Clark, C.W. (2010): *NIST Handbook of Mathematical Functions*. Cambridge University Press.

[24] Ureda, M.S. (2004): "Analysis of loudspeaker line arrays." In: *J. Audio Eng. Soc.*, **52**(5):467–495.

[25] Straube, F.; Schultz, F.; Weinzierl, S. (2015): "On the effect of spatial discretization of curved line source arrays." In: *Fortschritte der Akustik: Tagungsband d. 41. DAGA, Nürnberg*, 459–462.

[26] Straube, F.; Schultz, F.; Bonillo, D.A.; Weinzierl, S. (2017): "An analytical approach for optimizing the curving of line source arrays." In: *Proc. of 142nd Audio Eng. Soc. Conv., Berlin*, accepted after full paper review.

[27] Schultz, F.; Straube, F.; Spors, S. (2015): "Discussion of the Wavefront Sculpture Technology criteria for straight line arrays." In: *Proc. of 138th Audio Eng. Soc. Conv., Warsaw*, #9323.

[28] Straube, F.; Schultz, F.; Weinzierl, S. (2015): "Evaluation strategies for the optimization of line source arrays." In: *Proc. of 59th Intl. Audio Eng. Soc. Conf., Montreal*.

[29] L'Acoustics (january, 2016), "Variable curvature line source—behavior and optimization (training module, v1.1)." slide deck.

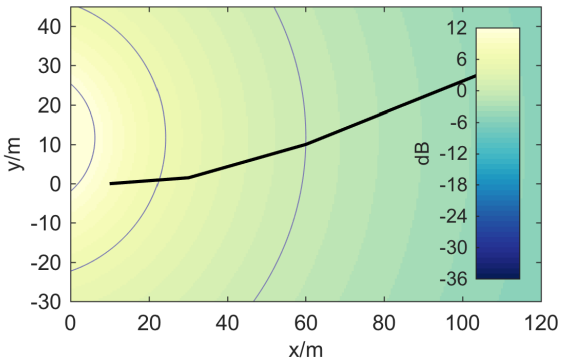

(a) SPL of a virtual point source at $\mathbf{x}_{\mathrm{PS}}/\mathrm{m} = (-11.8, 11.7, 0)^{\mathrm{T}}$ in the xy-plane. SPL relative to $\mathbf{x}_{\mathrm{Ref}}/\mathrm{m} = (60, 10, 0)^{\mathrm{T}}$. 6 dB steps for isobars in gray.

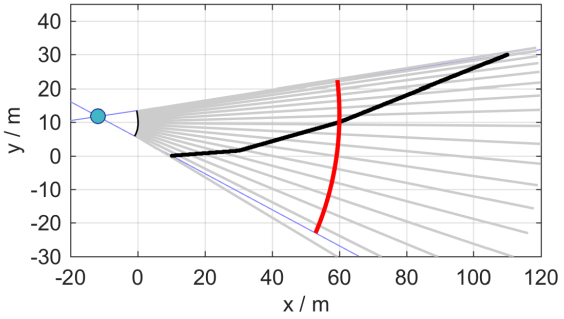

(b) Venue profile, LSA, virtual point source setup. Positions of amplitude correct synthesis (PCS) as red curve for **referencing to the specified reference point** $\mathbf{x}_{\mathrm{Ref}}/\mathrm{m} = (60, 10, 0)^{\mathrm{T}}$.

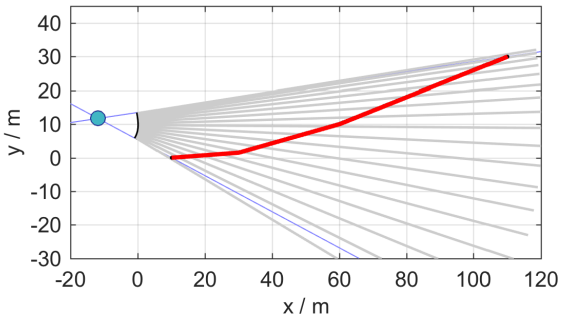

(c) Setup as Fig. 2b with positions of amplitude correct synthesis (PCS) as red curve for **audience line adapted referencing**.

Fig. 2: WFS of a virtual point source with an LSA for an amphitheater sound-reinforcement situation. Different WFS referencing schemes are applied in the subfigures.

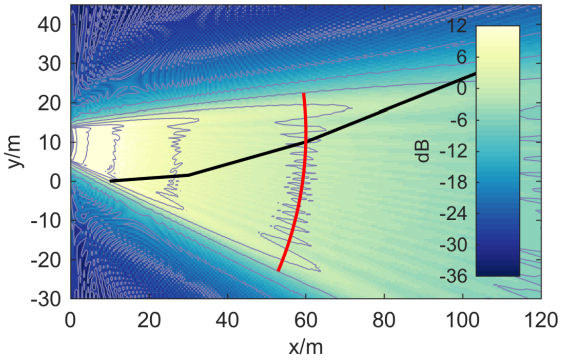

(a) SPL in *xy*-plane for 4 kHz. Positions of amplitude correct synthesis (PCS) as red curve. 6 dB steps for isobars in gray.

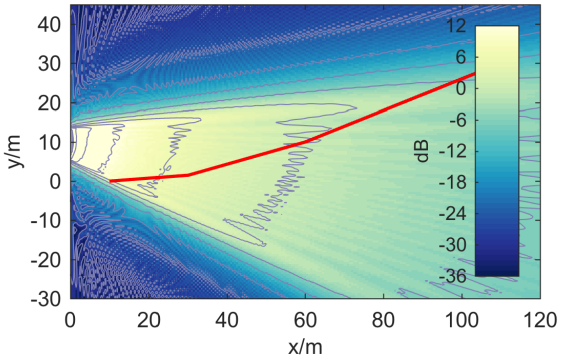

(b) SPL in *xy*-plane for 4 kHz. Positions of amplitude correct synthesis (PCS) as red curve. 6 dB steps for isobars in gray.

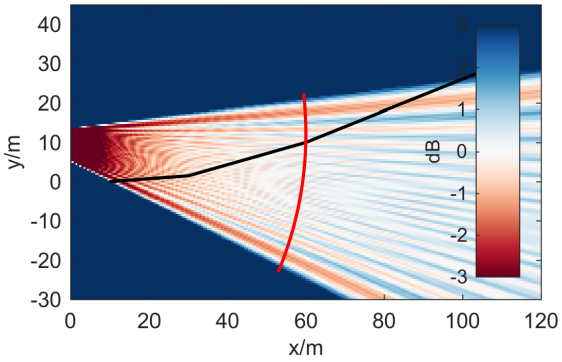

(c) Error measure: $20\log_{10}|P_{\mathrm{PS}}| - 20\log_{10}|P_{\mathrm{WFS,LSA}}|$ in *xy*-plane.

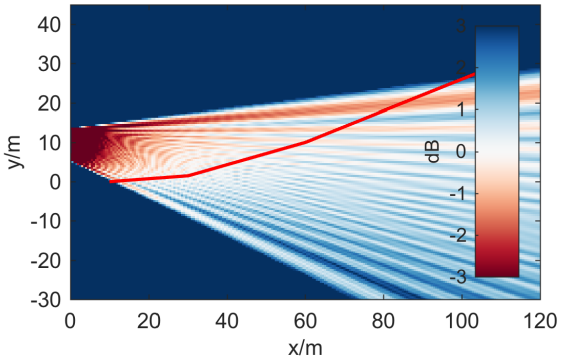

(d) Error measure: $20\log_{10}|P_{\mathrm{PS}}| - 20\log_{10}|P_{\mathrm{WFS,LSA}}|$ in *xy*-plane.

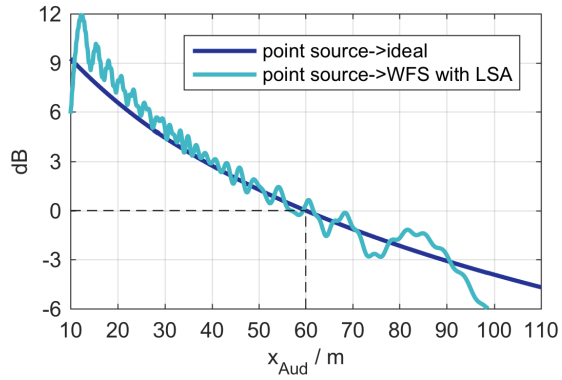

(e) SPL $20\log_{10}|P_{\mathrm{PS}}|$ and $20\log_{10}|P_{\mathrm{WFS,LSA}}|$ along audience line.

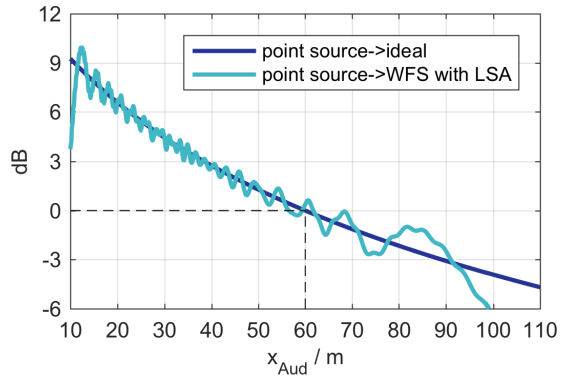

(f) SPL $20\log_{10}|P_{\mathrm{PS}}|$ and $20\log_{10}|P_{\mathrm{WFS,LSA}}|$ along audience line.

Fig. 3: WFS of a virtual point source with an LSA for an amphitheater sound-reinforcement situation. Left: referencing to $\mathbf{x}_{\mathrm{Ref}}/\mathrm{m} = (60, 10, 0)^{\mathrm{T}}$, right: audience line adapted referencing. Results for 4 kHz. Note that $D_{\mathrm{PS}}(\mathbf{x}_0, \omega)$ (17) is equivalent to (23) using DD_{dB}=0 dB. SPL normalized to point source level at $\mathbf{x}_{\mathrm{Ref}}$.

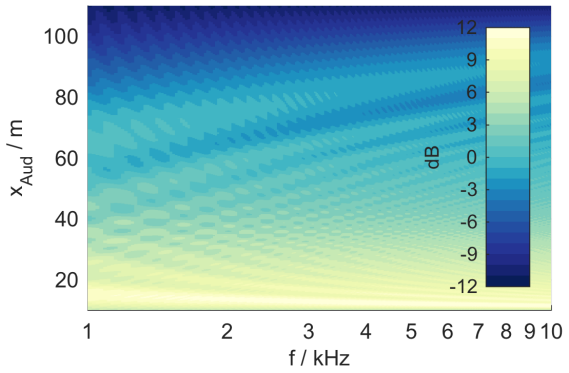

(a) Position index plot (PIP) $20\log_{10}|P_{\mathrm{WFS,LSA}}(\mathbf{x}_{\mathrm{Aud},m},\omega)|$ along audience line. SPL normalized to point source level at $\mathbf{x}_{\mathrm{Ref}}$.

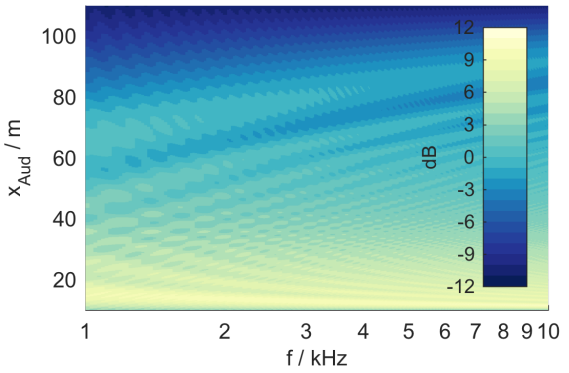

(b) Position index plot (PIP) $20\log_{10}|P_{\mathrm{WFS,LSA}}(\mathbf{x}_{\mathrm{Aud},m},\omega)|$ along audience line. SPL normalized to point source level at $\mathbf{x}_{\mathrm{Ref}}$.

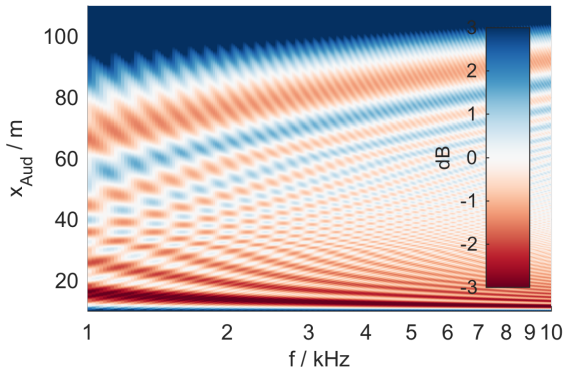

(c) Error measure: $20\log_{10}|P_{\mathrm{PS}}| - 20\log_{10}|P_{\mathrm{WFS,LSA}}|$ along audience line.

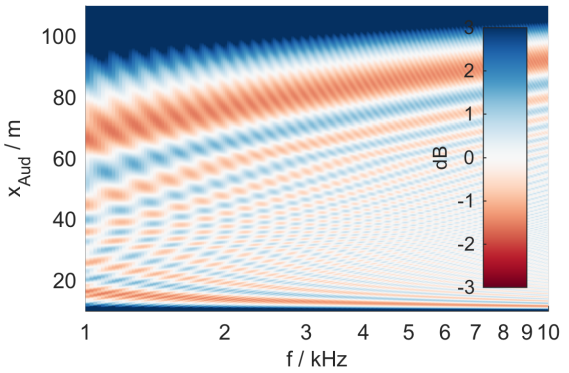

(d) Error measure: $20\log_{10}|P_{\mathrm{PS}}| - 20\log_{10}|P_{\mathrm{WFS,LSA}}|$ along audience line.

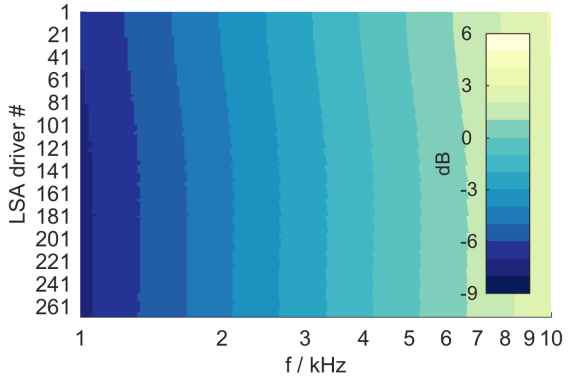

(e) Driving function index plot (DFIP) for (17), $20\log_{10}|D_{\mathrm{PS}}(\mathbf{x}_{0,i},\omega)|$.

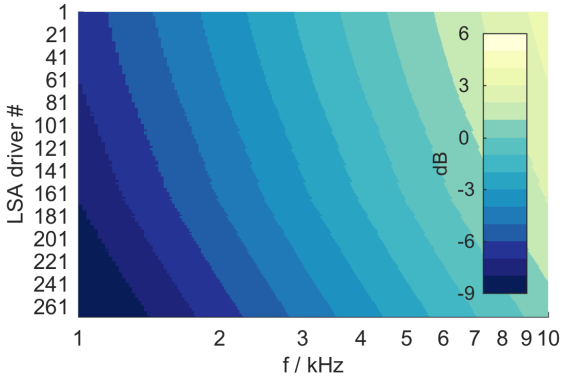

(f) Driving function index plot (DFIP) for (17), $20\log_{10}|D_{\mathrm{PS}}(\mathbf{x}_{0,i},\omega)|$.

Fig. 4: WFS of a virtual point source with an LSA for an amphitheater sound-reinforcement situation. Left: referencing to $\mathbf{x}_{\mathrm{Ref}}/\mathrm{m} = (60,10,0)^{\mathrm{T}}$. Right: audience line adapted referencing.

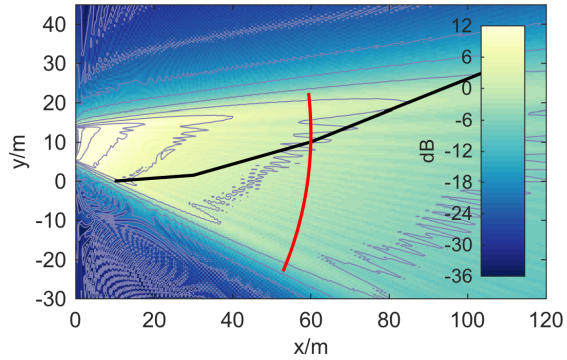

(a) SPL in *xy*-plane for 4 kHz. Positions of amplitude correct synthesis (PCS) as red curve. 6 dB steps for isobars in gray.

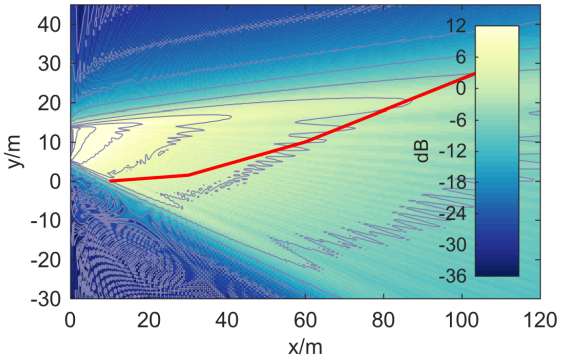

(b) SPL in *xy*-plane for 4 kHz. Positions of amplitude correct synthesis (PCS) as red curve. 6 dB steps for isobars in gray.

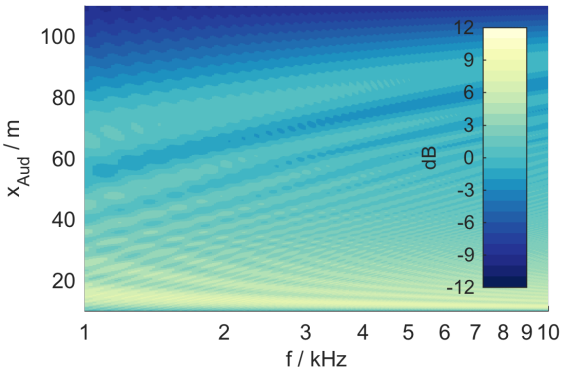

(c) Position index plot (PIP) $20\log_{10}|P_{\mathrm{WFS,LSA}}(\mathbf{x}_{\mathrm{Aud},m},\omega)|$ along audience line.

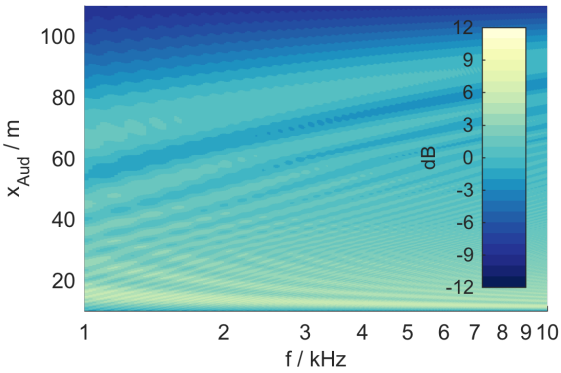

(d) Position index plot (PIP) $20\log_{10}|P_{\mathrm{WFS,LSA}}(\mathbf{x}_{\mathrm{Aud},m},\omega)|$ along audience line.

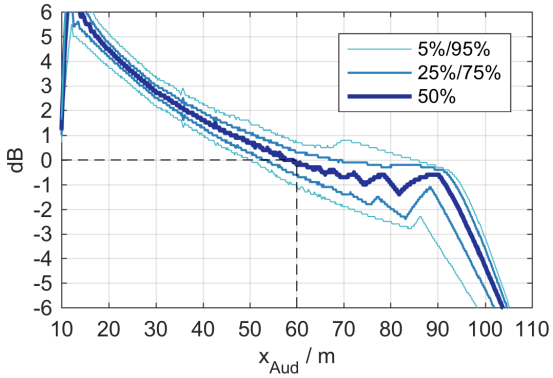

(e) Magnitude spectrum quantiles over frequency $L_{p,Aud,m}$

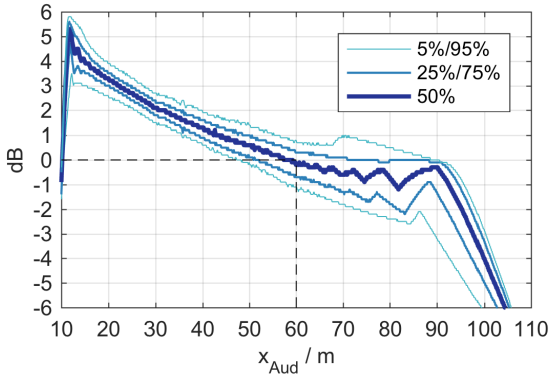

(f) Magnitude spectrum quantiles over frequency $L_{p,Aud,m}$

Fig. 5: WFS of a virtual directional point source with an LSA for an amphitheater sound-reinforcement situation. Left: referencing to $\mathbf{x}_{\mathrm{Ref}}/\mathrm{m} = (60,10,0)^{\mathrm{T}}$. Right: audience line adapted referencing. DD_{dB}=-10 dB results in 3 dB SPL loss per doubling the distance $|\mathbf{x}_{\mathrm{Aud}} - \mathbf{x}_{\mathrm{PS}}|$. SPL normalized to point source level at $\mathbf{x}_{\mathrm{Ref}}$.

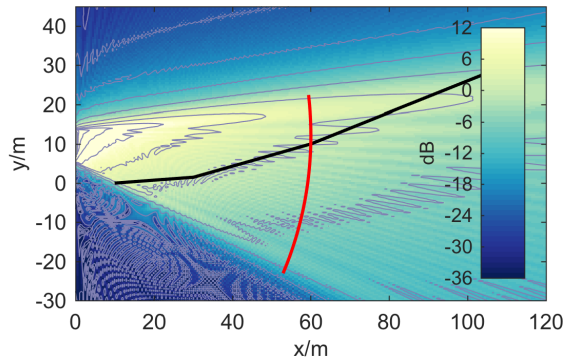

(a) SPL in *xy*-plane for 4 kHz. Positions of amplitude correct synthesis (PCS) as red curve. 6 dB steps for isobars in gray.

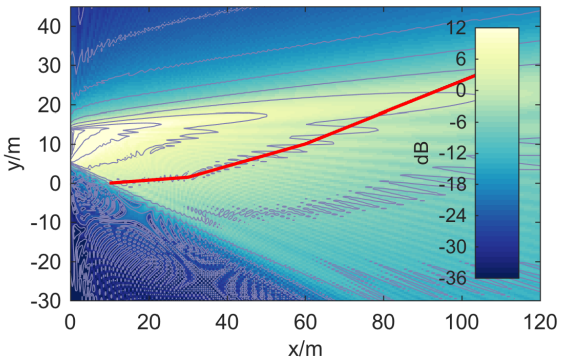

(b) SPL in *xy*-plane for 4 kHz. Positions of amplitude correct synthesis (PCS) as red curve. 6 dB steps for isobars in gray.

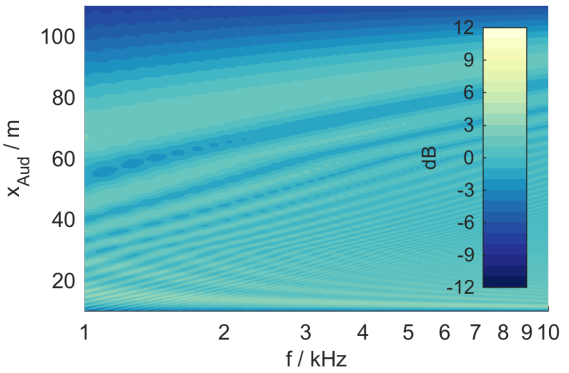

(c) Position index plot (PIP) $20\log_{10}|P_{\mathrm{WFS,LSA}}(\mathbf{x}_{\mathrm{Aud},m},\omega)|$ along audience line.

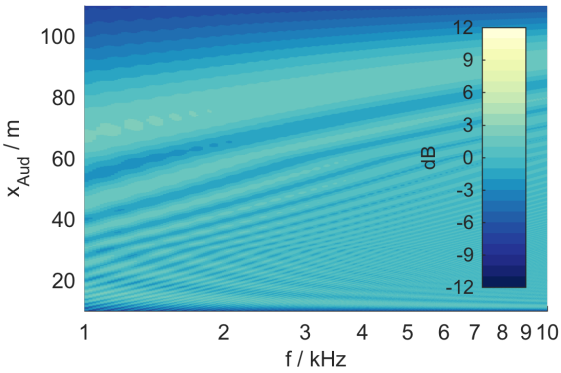

(d) Position index plot (PIP) $20\log_{10}|P_{\mathrm{WFS,LSA}}(\mathbf{x}_{\mathrm{Aud},m},\omega)|$ along audience line.

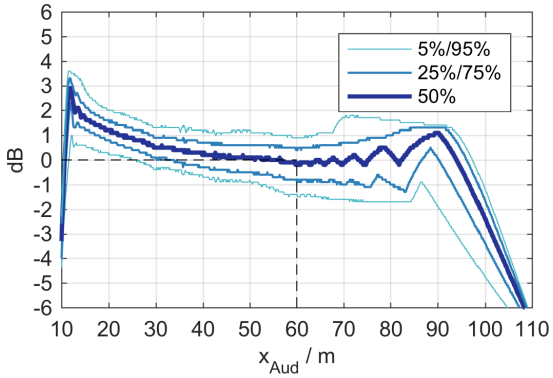

(e) SPL quantiles over frequency $L_{p,Aud,m}$

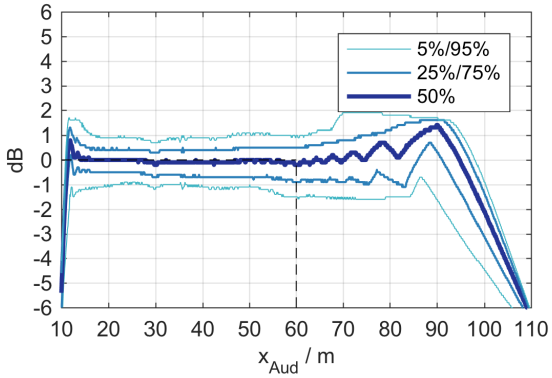

(f) SPL quantiles over frequency $L_{p,Aud,m}$

Fig. 6: WFS of a virtual directional point source with an LSA for an amphitheater sound-reinforcement situation. Left: referencing to $\mathbf{x}_{\mathrm{Ref}}/\mathrm{m} = (60,10,0)^{\mathrm{T}}$. Right: audience line adapted referencing. DD_{dB}=-20 dB results in 0 dB SPL loss per doubling the distance $|\mathbf{x}_{\mathrm{Aud}} - \mathbf{x}_{\mathrm{PS}}|$. SPL normalized to point source level at $\mathbf{x}_{\mathrm{Ref}}$.